

Results from the observation of extragalactic objects with the MAGIC telescope

D. Kranich on behalf of the MAGIC collaboration
ETH Zurich, CH-8093 Switzerland

In the last couple of years the Magic air Cherenkov telescope has made significant contributions to very high energy γ -ray astronomy. These include the detection of the galactic binary system LSI +61 303 and the observation of pulsed emission from the Crab pulsar. Extragalactic objects like the famous FSRQ 3C 279 and the LBL S5 0716+714 have both been detected during optical high states, and the radio galaxy M87 could be observed during an unexpected strong γ -ray outburst. Given its low energy trigger threshold (50 GeV) and fast repositioning time of less than 30s the Magic air Cherenkov telescope is particularly well suited for the observation of fast transient objects like AGN or GRBs. So far no GRB could be detected with Magic, however. In this paper we present selected highlights from recent MAGIC observations of extragalactic objects.

I. THE MAGIC TELESCOPE

The MAGIC Cherenkov telescope is located on the Canary Island La Palma. The telescope has a large parabolic Mirror of 234m², a 3.5° FoV camera with 577 enhanced QE PMTs and a 2 GS/s FADC system. Its design was optimized for a low 50 GeV trigger threshold and a fast repositioning time of 300° in 30 s. MAGIC has an $\sim 30\%$ enhanced duty cycle as observations are also carried out during twilight or the presence of moonlight. Further details on the telescope and its performance can be found in [1], [2] and [3]. A second telescope, MAGIC-II, which will significantly enhance the detector performance is about to be fully commissioned [4].

II. GAMMA RAY BURSTS

MAGIC started to follow-up GCN alerts in the beginning of 2005 and has observed more than 50 GRBs since then. Out of 23 GRBs observed during the last two years, 7 GRBs with accurate pointing position and weather condition were thoroughly analyzed. No detection, but upper limits for different energy regions could be made (Tab. I). Follow up observations on accessible GRBs started in between 1 and 3 minutes after the burst onset.



FIG. 1: The MAGIC telescope

TABLE I: Upper limits for selected GRBs at different energy bins, given in units of 10^{-10} erg cm⁻² s⁻¹.

observation time after T_0 in [s]	Energy bin [GeV]			
	80-125	125-175	175-300	300-1000
GRB080315				
160 \rightarrow 1716	–	0.16	0.18	0.05
1761 \rightarrow 5061	–	–	0.05	0.05
GRB080319A				
259 \rightarrow 1736	–	0.57	0.11	0.06
GRB080330				
91 \rightarrow 974	–	–	0.76	0.49
974 \rightarrow 1754	–	–	–	0.33
GRB080430				
4753 \rightarrow 11011	0.55	0.77	0.30	0.05
16912 \rightarrow 17968	7.76	6.59	2.45	0.92
GRB080603B				
5578 \rightarrow 7317	–	0.16	0.06	0.01
7497 \rightarrow 12357	–	0.05	0.12	0.03
GRB090102				
1161 \rightarrow 5181	2.30	1.61	0.34	0.04
5181 \rightarrow 9381	1.12	0.50	0.20	0.07
9861 \rightarrow 11241	–	1.02	0.30	0.20
11241 \rightarrow 12621	–	2.40	0.49	0.25
12621 \rightarrow 14841	–	–	0.40	0.11
GRB090113				
4603 \rightarrow 10063	0.54	0.99	0.10	0.08
10183 \rightarrow 13363	–	0.93	0.2 3	0.08

III. FSRQ 3C 279

The FSRQ 3C 279 is one of the brightest objects at all wavelengths and was the first blazar to be discovered at γ -rays [6]. It is also the first FSRQ found at VHE γ -rays [7] and, given its redshift of $z = 0.536$, the most distant VHE γ -ray emitter detected so far. Due to its large redshift 3C 279 is an important object to study the EBL photon field. The Magic observations

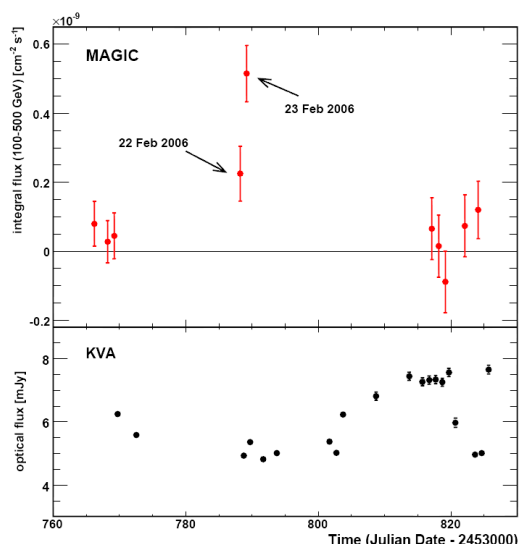


FIG. 2: VHE γ -ray (top) and optical R-band lightcurve (bottom) from 3C 279, taken in spring 2006.

which lead to the detection at 5.8σ were performed in spring 2006. The signal basically came from a single flare on February 23rd (Fig. 2). The optical and VHE γ -ray flux do not show correlated short-term behavior during the campaign. As the overall optical flux was about a factor 2 above the long-term baseline of 3 mJy, this data do also support some weak optical - VHE γ -ray correlation as found in other objects.

New observations after another optical outburst in January 2007 also led to a 5.2σ detection [8].

The MAGIC energy spectrum is well described by a pure power law with photon Index $\Gamma = 4.11 \pm 0.68$ (Fig. 3). The low level EBL corrected spectrum can be fitted by a one-zone SSC+EC model [11]. Taking into account quasi-simultaneous optical and X-ray data, however, suggests a multi-zone emission region (Fig. 4). Hadronic models also seem to describe the data well [12].

IV. BL LAC S5 0716+714

The low peaked BL Lac S5 0716+714 was observed with MAGIC for about 13h between November 2007 and April 2008. Both observations were triggered by strong optical flares seen by KVA. In November 2007 MAGIC follow up observations began 11 days after the trigger due to moon and bad weather constrains. The optical flux had already decreased significantly by then and no signal could be found. The April 2008 observations started 5 days after the trigger when the optical flux was still high (Fig. 5). The significance of the combined data was 5.8σ [13] mainly coming from the 2008 data set (giving 6.9σ). In 2008, the integral flux above 400 GeV was $F = 7.5 \pm 2.2 \cdot 10^{-12}$ ph/cm²/s

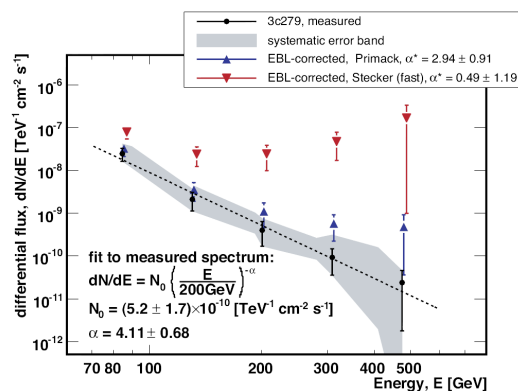


FIG. 3: MAGIC 3C 279 VHE γ -ray spectrum as obtained from the 2006 data. The red and blue points refer to the de-absorbed spectra using two different EBL models.

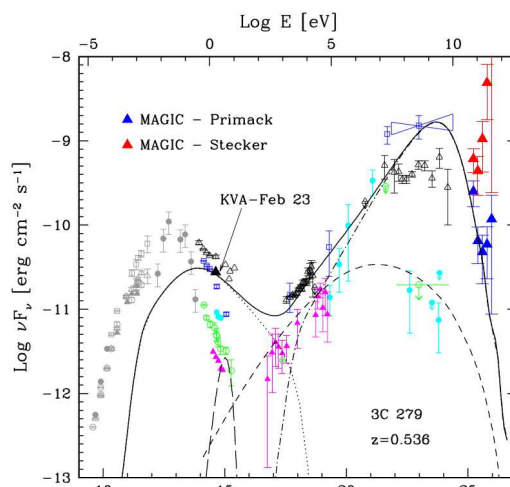


FIG. 4: Historical 3C 279 broad band SED (bottom) for the years 1991 to 2003 [9, 10] together with the 2006 MAGIC data points. The red and blue MAGIC points refer to the de-absorbed spectra using two different EBL models.

which corresponds to about 9% of the Crab Nebula flux. It should be noted that S5 0716+714 was also in a historical high state in X-rays [14] in April 2008.

S5 0716+714 is the third low peaked VHE Blazar after BL Lac (MAGIC) and W Comae (Veritas). The redshift was determined from the host galaxy as $z = 0.31 \pm 0.08$ [16] which makes S5 0716+714 the 2nd farthest VHE object detected so far. Due to the large redshift, the energy spectrum is rather steep with a photon index $\Gamma = 3.45 \pm 0.54$ (Fig. 6).

The broadband SED for the April 2008 data set is shown in Fig. 7. A simple one-zone SSC model (solid line) well describes the broad band SED, but predicts huge GeV fluxes. A structured jet model [17], shown as dashed line, would not require such large GeV fluxes and, in addition, would result in a photon index at GeV energies which is consistent with the one

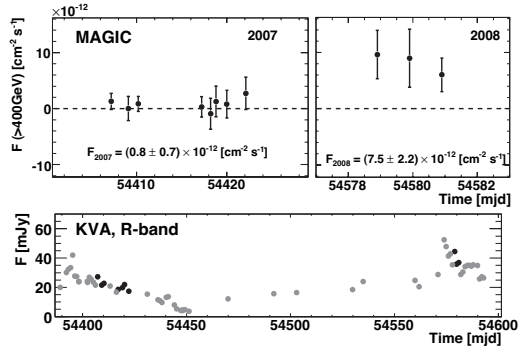


FIG. 5: The S5 0716+714 lightcurve in VHE γ -rays (upper panel) and optical (lower panel) as measured from November 2007 until April 2008. The optical data which was taken simultaneously with MAGIC are shown in black.

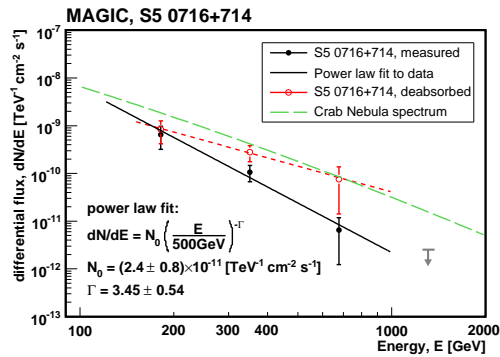


FIG. 6: S5 0716+714 energy spectrum as obtained from the 2008 data set. The de-absorbed spectrum was derived using the EBL model of [15] and assuming $z = 0.26$

measured by Fermi (blue bow tie in Fig. 7) during a presumably different intensity state.

V. MRK 501 MULTI-WAVELENGTH CAMPAIGN

Mrk 501 was observed between March and May 2008 as part of an extensive multiwavelength observation campaign covering radio (Effelsberg, IRAM, Medicina, Metsähovi, Noto, RATAN-600, VLBA), optical (KVA), UV (Swift/UVOT), X-ray (RXTE/PCA, Swift/XRT and Swift/BAT) and γ -ray (MAGIC, Whipple, VERITAS) energies. The duration as well as the energy coverage of this particular Mrk 501 campaign are rather unique. Mrk 501 was found in a low state of activity at about 20% the Crab Nebula VHE flux. Nevertheless, significant flux variations could be observed. In particular at X-rays but also, less pronounced, in γ -rays (Fig. 8). Overall Mrk 501 showed an increased variability when going from radio to γ -ray energies.

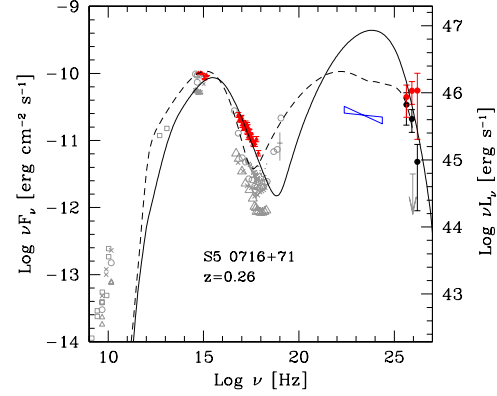


FIG. 7: S5 0716+714 SED for the 2008 data sample (red) and some historical data (gray). The gray arrow corresponds to the MAGIC upper limit derived from the November 2007 data sample. The result from a one-zone SSC model fit is shown as solid line. The dashed line corresponds to a spine-layer model fit as described in [17].

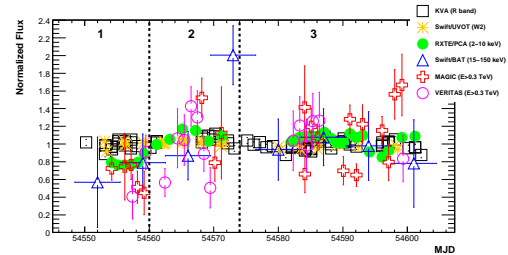


FIG. 8: Normalized Mrk 501 light curves as obtained for a selection of the instruments taking part in the campaign 2008. The vertical bars denote 1σ statistical uncertainties, and the horizontal bars the integration time of the observation.

Significant correlations between different energy bands have been found for the pairs RXTE/PCA - Swift/XRT (DCF: 0.87 ± 0.28) and also, less significant, RXTE/PCA (or Swift/XRT) with VHE γ -rays (DCF: 0.5 ± 0.19). No hints for possible time-lags have been found. The correlation analysis was, however, strongly affected by the modest flux variability and / or the large flux errors. The broadband spectral energy distribution during the two different emission states of the campaign is well described by a homogeneous one-zone synchrotron self-Compton model [18] as shown in Fig. 9. The high emission state was satisfactorily modeled by increasing the amount of high energy electrons with respect to the low emission state. This parameterization is consistent with the energy-dependent variability trend observed during the campaign. The model parameter values for the different emission states are given in table II.

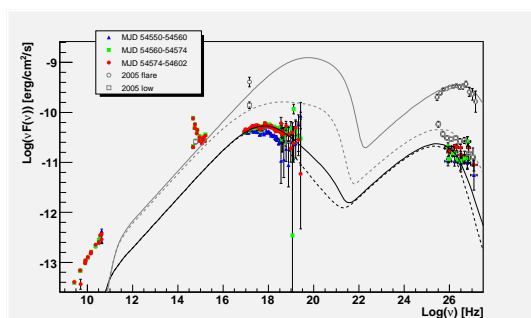


FIG. 9: Broadband SED for Mrk 501 as obtained during the 2008 MWL campaign in comparison to low and high states from 2005. The results from a SSC model fit to the low state 2008 data (dot-dashed curve), the high state 2008 data (heavy-dashed curve), the 2005 low state (light-dashed curve) and the 2005 high state (solid line curve) are also shown.

TABLE II: The SSC model parameters used to describe the broadband SED for different flux states of the Mrk 501 MWL campaign in 2005 and 2008.

SSC parameters	2008 high	2008 low	2005 high	2005 low
γ_{break}	$2.6 \cdot 10^5$	$2.2 \cdot 10^5$	$1.0 \cdot 10^6$	$1.0 \cdot 10^5$
e^- slope n_1	2.0	2.0	2.0	2.0
e^- slope n_2	3.9	4.2	3.9	3.2
mag. field B [G]	0.19	0.19	0.23	0.31
density K [cm^{-3}]	$1.8 \cdot 10^4$	$1.8 \cdot 10^4$	$7.5 \cdot 10^4$	$4.3 \cdot 10^4$
Radius R [cm]	$3 \cdot 10^{15}$	$3 \cdot 10^{15}$	$1 \cdot 10^{15}$	$1 \cdot 10^{15}$
Doppler factor δ	12	12	25	25

VI. RADIO GALAXY M 87

M 87 is a nearby Radio Galaxy located in the center of the Virgo cluster and was the first Radio Galaxy to be detected at VHE γ -rays [19]. In 2008 a joint campaign involving all three next generation Cherenkov telescopes (H.E.S.S., MAGIC and VERITAS) observed M 87 for in total 120h from January until May. In February, MAGIC detected a strongly increased emission from M 87 and triggered MWL ob-

servations with radio, X-ray and extended VHE coverage [20]. The data show evidence for a correlated radio and VHE γ -ray emission and allowed to constrain the origin of the VHE γ -ray emission to the immediate vicinity of the central black hole. There is a dedicated presentation [21] on this campaign.

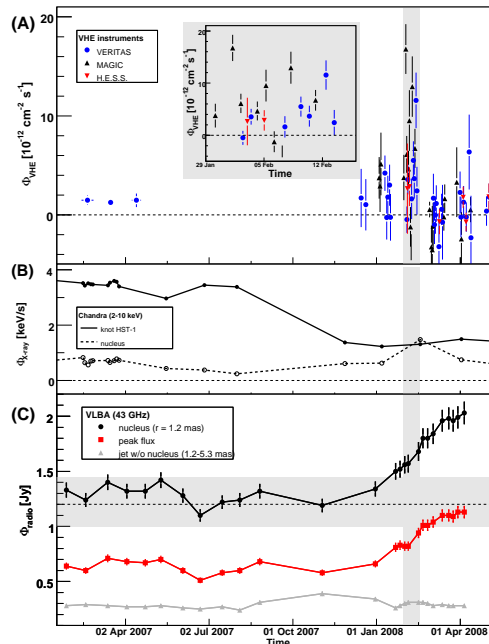


FIG. 10: M87 light curves from 2007 to 2008 at VHE γ -rays (top, H.E.S.S., MAGIC and VERITAS), X-rays (middle, Chandra) and radio (bottom, 43 GHz, VLBA). The inset in the top panel shows a zoom of the flare in February 2008.

Acknowledgments

We thank the Instituto de Astrofísica de Canarias for the excellent working conditions at the Observatorio del Roque de los Muchachos in La Palma. The support of the German BMBF and MPG, the Italian INFN and Spanish MCINN is gratefully acknowledged.

[1] C. Baixeras et al., Nucl. Instrum. Meth., A518, 188, 2004
 [2] J. Cortina et al., in Proceedings of the 29th International Cosmic Ray Conference, Pune, India, 5, 359, 2005
 [3] J. Albert et al., ApJ, 674, 1037, 2008
 [4] A. Moralejo, this proceeding, 2009
 [5] M. Garzaczzyk et al., arXiv:0907.1001, 2009

[6] R.C. Hartman et al., ApJ, 385L, 1, 1992
 [7] J. Aliu et al., Science 320, 1752, 2008
 [8] K. Berger et al., arXiv:0907.1046v1, 2009
 [9] L. Ballo et al., ApJ, 567, 50, 2002
 [10] W. Collmar et al., in Proceedings of the 5th INTEGRAL Workshop ESA SP-552, p. 555, 2004
 [11] L. Maraschi and F. Tavecchio, ApJ 593, 667, 2003
 [12] M. Boettcher et al., arXiv:0810.4864, 2008

- [13] H. Anderhub et al., ApJ 704, L129, 2009
- [14] P. Giommi et al., ATel 1495, 2008
- [15] A. Franceschini et al., A&A 487, 837, 2008
- [16] K. Nilsson et al., A&A 487, L29, 2008
- [17] F. Tavecchio and G. Ghisellini, MNRAS 394, 131, 2009
- [18] F. Tavecchio et al., ApJ 554, 725, 2001
- [19] F. Aharonian et al., A&A 401, L1, 2003
- [20] V.A. Acciari et al., Science 325, 444, 2009
- [21] R. Wagner, this proceeding, 2009